Technical report, IDE1109, March 2011

Performance Analysis and Link Design of Long Haul Coherent Optical OFDM Systems

Master's Thesis in Electrical Engineering

Ayhan Yazgan

School of Information Science, Computer and Electrical Engineering

Halmstad University

Performance Analysis and Link Design of Long Haul Coherent Optical OFDM Systems

Master's thesis in Electrical Engineering

School of Information Science, Computer and Electrical Engineering
Halmstad University
PO Box 823, S-301 18 Halmstad, Sweden

March 2011

Preface

I would like to thank my supervisor Dr. Jörgen Carlsson, Professor Hakan Pettersson and Dr. Lars Landin for their precious time and help. I am extremely glad that they made it possible for me to have such a high level education. I would like to thank Emil Nilsson for his continuous help even he was so busy. My thanks to Eva Strid Andersson for her support whenever I need. Above all I would like to mention Halmstad University and Karadeniz Technical University. Their support is gratefully acknowledged.

Ayhan Yazgan
Halmstad University, March 2011

Abstract

Orthogonal Frequency Division Multiplexing (OFDM) is a suitable solution due to its many advantages known in wireless communications. On the other hand, optical communications is also used as a backbone to transmit and receive large data rates with economical and good performance. Recently, fiber optical communication and OFDM method are combined to obtain both advantages in a communication link. Coherent optical OFDM (CO-OFDM) has recently been proposed against the chromatic dispersion effect in electrical domain. According to the ITU-T standards there are 111 channels (C and L bands) can be used (191.4 to 185.9 THz) at 50 GHz spacing. Thanks to Wavelength Division Multiplexing, even we use only one RF carrier, we can reach 1.7 Tb/s (111*16 Gb/s) using only one optical cable and utilizing C and L bands. In this research, CO-OFDM technique is modeled and simulated by designing a Monte Carlo simulation. In this simulation, dispersion, data rate, SNR-BER and BER-Distance variations are calculated and results are given in graphical forms. These graphics show the performance of the CO-OFDM system in 5, 8 and 16 Gb/s at different distances for one RF carrier and one optical carrier. It is also shown that how to get 64 Gb/s data rate using the same structure with one optical carrier.

Abbreviations

a : Fiber core diameter
Ac(t) : OFDM carrier amplitude
arg : Symbol phase angle
APD : Avalanche Photodiode
B : Magnetic field vector
BW : Bandwidth
BWOFDM : Bandwidth of an OFDM symbol
BER : Bit Error Rate
BPSK : Binary Phase Shift Keying
c : Light velocity in vacuum
CO-OFDM : Coherent Optical OFDM
CP : Cycle Prefix
DFT : Discrete Fourier Transform
D_t : Chromatic Dispersion Parameter
D_{PMD} : Polarization Mode Dispersion parameter
E : Electric field vector
E(t) : Time dependent Electric field
Eg : Band gap energy
FFT : Fast Fourier Transform
F_n : Amplifier noise figure
F_A : Excess noise factor
f_L : Laser frequency
f_k : k^{th} subcarrier of OFDM symbol
f_s : Sampling frequency
GI : Guard interval
G^{th} : Thermal Noise
GVD : Group velocity dispersion
I_d : Dark current
IDFT : Inverse Discrete Fourier Transform
IEEE : Institute of Electrical and Electronics Engineers
IF : Intermediate frequency
IFFT : Inverse Fast Fourier Transform
H : Magnetic field strength
h : Planck’s constant
h_k : Frequency response of k^{th} component of the channel
ICI : Intercarrier Interference
ISI : Intersymbol Interference
J : Current density
k_B : Bolzmann’s constant
L : Link distance
L_{max} : Maximum Link Distance
M : Multiplying factor (APD gain)
MIMO : Multiple Input Multiple Output
MZM : Mach Zehnder Modulator

n : Refractive index
n_{ik} : The noise component of kth subcarrier of ith symbol
NA : Numerical aperture
NRZ : None return to zero
N_{SC} : The number of OFDM subcarrier
N_{SD} : The number of OFDM data subcarrier
N_{SEMBOL} : The number of OFDM symbol
N_{SP} : The number of OFDM pilot subcarrier
OFDM : Orthogonal Frequency Division Multiplexing
OOK : On-Off keying
OSA : Optical Society of America
OTR : Optical to RF modulation
PIN PD : PIN photodiode
PD : Photodiode
R : Responsivity
R_L : Load resistance
RF : Radio Frequency
RTO : RF to Optical Modulation
RZ : Return to zero
SNR : Signal to Noise ratio
SSMF : Standart Single Mode Fiber
T_{CP} : Cycle Prefix duration
TE : Transvere Electric
TM : Transvere Magnetic
T_S : Sampling Period
T_{SYM} : OFDM symbol duration
T_U : Useful symbol duration
v : Light velocity in fiber optic cable
WAN : Wide Area Network
x_{ik} : The component of kth subcarrier of ith symbol at transmitter output
y_{ik} : The component of kth subcarrier of ith symbol at receiver input
x_{ik}^{fs} : The component of kth subcarrier of ith symbol after laser phase noise compensation at receiver
$\bar{\varphi}_i$: Estimated constant laser phase drift
φ0 : Constant phase component
φ(t) : Time dependent phase component
φi : Laser phase drift for ith component
$\bar{\phi}_D(f_k)$: Subcarrier phase component
φc(t) : Time dependent phase component for a subcarrier
$\varphi_D(k)$: Chromatic dispersion dependent phase component
λ_L : Laser wavelength
λc : Cut off wavelength
β : Phase constant
β_2 : GVD parameter

α : Attenuation constant
$\nabla \times$: Rotation
$\nabla \cdot$: Divergence
ε_o : Dielectric constant of medium
μo : Magnetic permeability of medium
ρv : Volume charge density
Δf : Frequency difference
Δf_L : Laser bandwidth
$\Delta\lambda$: Wavelength difference
$\Delta\lambda_L$: Laser wavelength difference
θc : Refraction angle
α_c : Acceptance angle of fiber
σ : Pulse spreading
δ_{nm} : Kronecker Delta

Contents

PERFORMANCE ANALYSIS AND LINK DESIGN OF LONG HAUL COHERENT OPTICAL OFDM SYSTEMS

1 INTRODUCTION

Fiber optical communication has been growing rapidly over the past twenty years. For several years now, optical fiber communication systems are being extensively used all over the world for telecommunication. Optical communications offer advantages of ultrahigh speed and highly reliable information transmission. The first ideas of applications of light guiding in glass fibers date from the late 1920's. They were all about image transmission through a bundle of fibers. A breakthrough happened in the beginning of the 1950's with the idea and demonstration that cladding the fibers would help light transmission, by facilitating total internal reflection. The invention of the laser in the early 1960s (Nobel Prize in 1964 to C. H. Townes, N. G. Basov, and A. M. Prokhorov) gave a new boost to the research in optical communication. Shortly after the pulsed laser demonstrated in ruby by T. H. Maiman, A. Javan built the first continuous wave laser using a mixture of He and Ne gas. Semi-conductor lasers appeared almost at the same time, but were at first not so practical, since they required high currents and could not work at room temperature. A few years later, the introduction of heterostructures (Nobel Prize in 2000 to Z. I. Alferov and H. Kroemer) enabled operation at room temperature, making them ideal light sources for optical communication. The tremendous breakthrough came out by Charles K.Kao with the suggestion of using silica as a medium for light transmission (Nobel Prize in 2009 with one half to Charles K. Kao and with Willard S. Boyle and George E. Smith sharing the other half). The Nobel Prize in Physics 2009 was divided, one half awarded to Charles K. Kao "for groundbreaking achievements concerning the transmission of light in fibers for optical communication", the other half jointly to Willard S. Boyle and George E. Smith "for the invention of an imaging semiconductor circuit – the CCD sensor".

Orthogonal frequency division multiplexing (OFDM) has recently received a lot of attention to struggle RF microwave multipath fading, and has been extensively implemented in various digital communication standards such as WIMAX, LTE, WIFI [1]. The key idea behind OFDM is to split a high-data rate data-stream into a number of low-rate data-streams that are transmitted simultaneously over a number of subcarriers. OFDM offers good spectral efficiency and efficient elimination of subchannel and symbol interference using the Inverse Fast Fourier Transform (IFFT) for modulation and Fast Fourier Transform (FFT) for demodulation, which does not require any equalization. The symbol duration of these low-rate data-streams is made substantially larger, with a goal to increase the robustness of a system to chromatic dispersion. In order to meet the increasing demand for bandwidth, novel robust and efficient modulation techniques are required not only for short network links but also for the backbone. Recently, an equivalent optical-domain multi-carrier format, named Coherent Optical OFDM (CO-OFDM) has been proposed as an impressive technique for long haul transmission to remove inter-symbol interference (ISI) caused by chromatic dispersion in fiber optical medium [2]. In a CO-OFDM system, optical Mach–Zehnder modulators (MZMs) are used to up-convert the OFDM signal from the RF domain to optical domain. In the receiver side we use coherent balanced receivers to down-covert the OFDM signal from optical domain to the RF domain. In the mean time, incoherent optical OFDM (IO-OFDM) has also been proposed independently, and has been shown to have similar dispersion tolerance with a much simpler detection scheme. However, the CO-OFDM is superior to IO-OFDM in spectral efficiency, OSNR requirement, and Polarization Mode Dispersion (PMD) insensitivity [3, 4]. On the other hand, the main challenge of CO-OFDM is that the phase noise of the local oscillator must be compensated for [4]. In conventional

CO-OFDM systems, phase noise is compensated by estimating the local oscillator (LO) offset using the cyclic prefix or preambles. In this work we focused on the dispersion compensation aspect of the new method called CO-OFDM. Attenuation factor of fiber cable in C band also has to be taken into consideration especially for link design. But this effect can be eliminated using Erbium Doped Fiber Amplifiers (EDFA's) or Raman amplifiers with properly chosen pump power and cable length to get the minimum nonlinearity. On the other hand dispersion effect can not be eliminated as simple as the attenuation. For long haul communication systems repeaters have to be used to get rid of dispersion effect. We replace these expensive components with CO-OFDM method with its flexibility for changing some properties. In the field of COOFDM long haul transmission, the first transmission experiment has been reported for 1000 km SSMF transmission at 8 Gb/s, and more CO-OFDM transmission experiment have rapidly been reported by S. Jensen et. al. for 4160 km SSMF transmission at 20 Gb/s [5, 6]. Direct detection systems have also been worked by J. M. Tang and K. Alan Shore with their work 30 Gb/s Signal Transmission Over 40-km Directly Modulated DFB-Laser-Based Single Mode Fiber Links Without Optical Amplification and Dispersion Compensation [7]. Supporting electronic equalizers, data rates can reach up to 100 Gb/s as reported by Chris R. S. Fludger et. al. with their work Coherent Equalization and POLMUX-RZ-DQPSK for Robust 100-GE Transmission [8]. Because of electronic materials are getting more expensive in higher data rates, we avoid using an electronic equalizer. In this work we investigate CO-OFDM performance over long haul fiber optical links at different data rates and different dispersion parameters using only one RF carrier and one optical carrier. We use Binary Phase Shift Keying (BPSK) as a digital modulation format to reach 16 Gb/s data rate. It is known that 50 GHz spacing is being used for very high density wavelength division multiplexing (VHDWDM) [9]. To realize it, the system can be upgraded by using Quadrature Phase Shift Keying (QPSK) with two suitable RF carriers instead of one. In this case, we reach up to 64 Gb/s without using any equalizer. On the other hand communication system will be more sensitive to noise. Finally, we demonstrate the maximum link distance of CO-OFDM transmission system for different signal to noise ratio (SNR) values without dispersion compensation. Furthermore a small number of CO-OFDM link designs are also constituted.

1.1 Goal

The objective of this project is to investigate and simulate the new technique named CO-OFDM for long haul fiber optical communication systems up to 1.7 Tb/s. For that reason a Monte Carlo simulator is developed using Microsoft Visual C++ programming tool [10-13]. Then this simulator is upgraded to get the new results which describe the relation between BER and the link distances under the condition of constant signal to noise ratio.

2 BACKGROUND

Because of the reliability, high capacity and security, optical communication is now the backbone of the whole communication systems in the world. Basically optical transmitter, optical receiver and the fiber part are the heart of the fiber optical communication system.

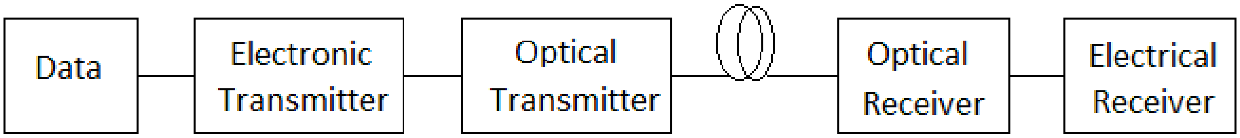

Fig. 1. Fiber optical communication system basic block diagram

Physically the basic theory of all parts is strongly related the principle of the photon-electron interaction. There are basically three processes for interaction between a photon and an electron in a solid material. These are absorption, spontaneous emission and stimulated emission. An atom in state E_1 absorbs the photon and thereby goes to the excited state E_2. The change in the energy state is the absorption processes shown in Fig. 2a and given in Eq.1. The excited state of the atom is unstable. After a short time, without any external stimulus, it makes a transition to the ground state, giving off a photon of energy hf_{21}. This process is called spontaneous emission. When a photon has energy hf_{21} hits against an atom, while it is in the excited state, the atom can be stimulated to make a transition to the ground state and gives off a photon of energy hf_{21} which is in phase with the incident radiation. This process is called stimulated emission. The radiation from stimulated emission is monochromatic because each photon has precisely an energy hf_{21}. It is also coherent because all photons emitted are in phase. If it is assumed that the instantaneous populations of E_1 and E_2 are n_1 and n_2 respectively, under thermal equilibrium the population is calculated with the Eq. 2 (if the condition E_2- E_1> 3 kT is satisfied) called Boltzmann distribution. It is also well known that in the steady state “spontaneous emission rate + stimulated emission rate = absorption rate” [14].

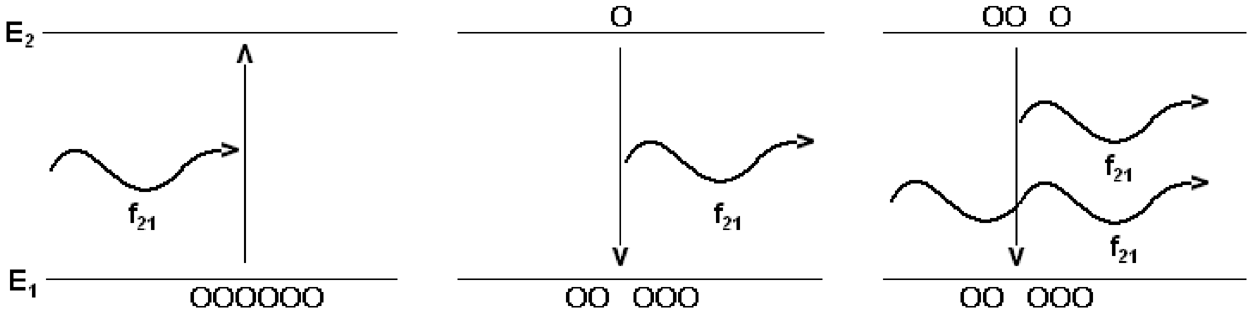

(a) **(b)** **(c)**

Fig. 2. (a) absorption, (b) spontaneous emission, (c) stimulated emission

$$E_2 - E_1 = \frac{hc}{\lambda_{21}} \tag{1}$$

$$\frac{n_2}{n_1} = \exp\left(-\frac{hf_{21}}{kT} \right) \qquad (2)$$

2.1 Optical Transmitters

The main part of the transmitter is the light source. Because, the only way to convert electrical signal into optical signal is to use a light source. Basically there are two kind of light source can be used. One of them is light emitting diode and the other one is laser diode. Both are produced direct band gap materials or their different compositions. The reason is that these kinds of materials do not need crystal momentum change. So when an electron recombines with a hole, the result is release of radiation that is called light such as GaAs. On the other hand indirect band gap materials release this energy as heat such as Ge or Si. That is why a transistor is warming up when the current is increased. To have a high device efficiency, heterojunctions must be used instead of using homojunctios. In this case the device is made from different types of semiconductor materials, each type having a different energy gap. At the end of this process we have the confinement of electron hole recombination within a highly restricted active region and the conduction of radiated light in one direction. For the confinement of electron hole recombination a semiconductor with a small energy gap is placed between the two layers of substrate semiconductor with the larger energy gap. For example GaAs has 1.42 eV band gap can be put into place between the AlGaAs layers whose band gap is 1.92 eV. Different wavelength values can be obtained by using different composition of materials as showed in Table 1. If it is considered from the point of view of long haul communications, laser diode has some crucial advantages over LED such as narrower spectral width, less dispersion-induced signal distortion, higher fiber coupling efficiency and greater transmission distance. For that reason, laser diodes are assumed as the unique transmitter source, in this work [15].

Table 1. Bang gap energy and wavelengths of popular semiconductors at 300 K

Material	Band gap energy E_g (eV)	Wavelength (nm)
Ge	0.775	1610
Si	1.17	1067
GaAs	1.424	876
InP	1.35	924
InGaAs	0.75-1.24	1006-1664
AlGaAs	1.42-1.92	650-879
InGaAsP	0.75-1.35	924-1664

2.1.1 Laser Diodes

Laser diode is an important part of the transmitter module of the optical communication systems. Especially semiconductor LD differs from other LD in that it is small and easily modulated at high frequencies. Semiconductor LD developed in the 1970s, have found vast commercial applications in CD players. With the advent of commercial optical fiber, such LD radiation properties as brightness, directivity, narrow spectral width and coherence made them the best light source for long haul fiber optical links. For the lasing action, stimulated emission is an indispensable factor. To enhance stimulated emission over spontaneous emission, we must have a very large photon-field energy density. To achieve this density, an optical resonant cavity is used to increase the photon field. If stimulated emissions of photons are to dominate over the absorption of photons, then we have higher electron density in E_2 level than the E_1 level. This condition is very important and called as population inversion. Today's technology support the channel separation for the DWDM systems is about 50 GHz. It can be seen from the Eq. 3 that even 0.1 nm spectral width is not acceptable. This requirement force designers to make some novelties on this field such as Vertical-cavity surface-emitting lasers (VCSEL), quantum-well lasers that have 4 to 20 nm of active region thickness with more efficient current to light conversion and distributed –feedback laser diodes [14, 15].

$$\Delta f = -\frac{c}{\lambda^2}\Delta\lambda \tag{3}$$

To get the exact band gap energy value, we can use different semiconductors and their compounds. There so many works on this field. Therefore the bandgap energy against the lattice constant for various III-V group semiconductors and their compounds can be easily investigated [16].

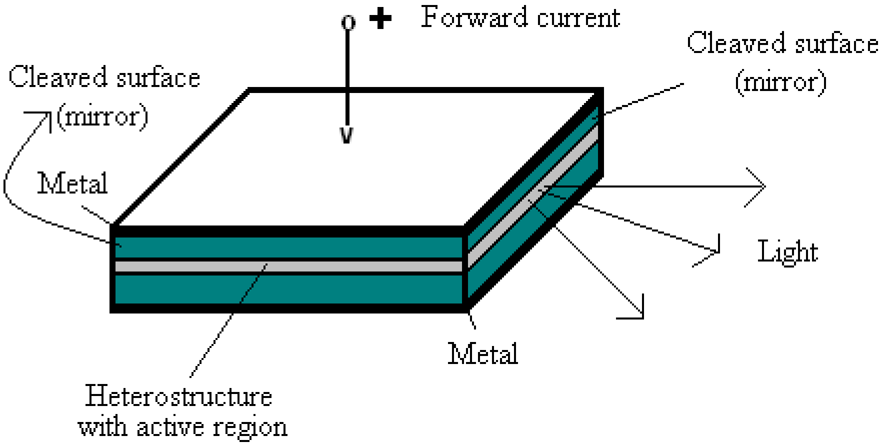

Fig. 3. Basic structure of a laser diode.

The basic construction of an LD is demonstrated in Fig. 3. Except for two important differences, an LD is similar to an LED. First, the thickness of an active region in a laser diode is very small, typically on the order of 0.1 μm. Second, laser diodes' both surfaces are cleaved to make them act as mirrors. Actually there is no physically mirror at two end surfaces. The two cleaved surfaces themselves form a resonator with length L. A resonator can support only one wave with a certain wavelength, the wave that forms a standing-wave pattern. This physical requirement is shown in Eq. 4 where L is the distance between mirrors and N is an integer. Because N can be N+1, N+2 and so on, this resonator can support different wavelengths. Wavelengths selected by a resonator are called longitudinal modes. The active medium provides gain within only small range of wavelengths because of the condition given in Eq. 5. So only several resonant wavelengths that fall within the gain curve might be radiated. It can be seen in Eq. 6 that spacing between two adjacent longitudinal modes λ_N- λ_{N+1} can be calculated. For example for a resonator L=0.6 mm and λ=1550 nm, λ_N- λ_{N+1} calculated 2 nm. Assuming the line width of a gain curve is equal 5 nm , it can be easily seen that this active medium can support two longitudinal modes. To reduce the spectral width, we need to make a laser diode radiate only one longitudinal mode. This has been done with distributed-feedback (DFB) laser diodes [14, 15].

$$\frac{2L}{\lambda} = N \tag{4}$$

$$\lambda < \frac{hc}{Eg} \tag{5}$$

$$\lambda_N - \lambda_{N+1} \approx \frac{2L}{N^2} = \frac{\lambda^2}{2L} \tag{6}$$

2.1.2 Optical Modulators

Modulators are being used in fiber optical communication system can be divided into two groups. One of them is internal modulator and second one is external modulators. Internal modulators change the intensity of radiated power from minimum to maximum and vice versa. But this effect increase the chirp effect is known as the fast variations of laser’s peak radiating frequency in response to a change in driving modulation current. Second negative effect of using an internal or direct modulator is bandwidth restriction. Both negative effects can be eliminated by using an external modulator [12]. Most of modern optical communication systems use MZM’s as an external modulator, especially OFDM systems. Because, theoretical analysis and numerical simulation results show that at the optimum operation bias point of π for MZM, the OFDM signal incurs minimum excess modulation insertion loss and Q penalty from nonlinearity [12]. Nowadays scientists who are working in this area, interested in nonlinearity effect for CO-OFDM systems [13, 17]. The principle of a MZM modulator can be explained as follows. A change in the input voltage level changes the strength of the electrical field across the waveguide. The change of electrical field changes the refractive index of LiNbO3. So velocity of light and phase difference between input and output signals are also changed. MZM modulators can be configurated as amplitude or phase modulators [18].

2.2 Optical Receivers

The most important part of the receiver is photodedector. Actually a photodedector converts light into electric current. We can easily say that a photodedector does just opposite thing what a light emitting diode does. Basically semiconductors have two energy bands separated by a forbidden area. The valence band has lower energy than the conduction band. At conduction band electrons can move easily but at the valence band they can not. If we keep electrons at conduction band then we can get more current. To achieve this result we need to pass the energy gap inside the semiconductor. So when a photon, has energy greater than the band gap, strikes the depletion region of the semiconductor, it is absorbed and its energy separates an electron from its hole. The separated hole and electron are attracted by negative and positive potentials that we applied before. This procedure explains the basic theory of optical receivers. At the end of this procedure, the current called I_p is produced as it can be seen in Fig. 4. The external voltage that is applied must be reverse bias in order to get only photo current. This effect is very important to get an efficient receiver. Furthermore there are several advantages to apply this reverse voltage. First of all this reverse voltage eliminates the dark current which stands for the current is produced by a photodiode without light. Secondly it improves the response of a photodiode. Thirdly this reverse voltage prevents recombining electrons and holes in the depletion region again. Because the separation time of these carriers is much less than their recombination lifetime because of the reverse voltage [15].

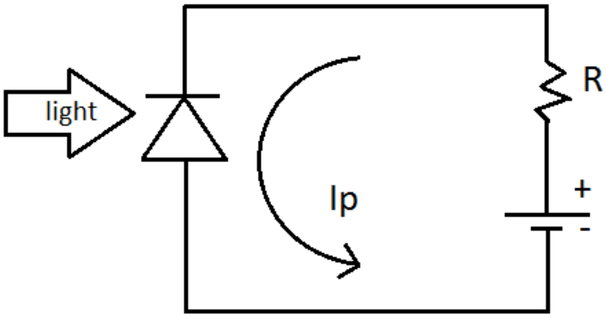

Fig. 4. Basic structure of a broad-area of a laser diode

One of the important parameter of the photodiode is the responsivity which is describing how a photodiode converts light into an electrical signal. This parameter is shown as R and the unit of it is A/W. But it can not be said that the more light power we have, the more electric current we get. Because, every photodiode has a saturation limit. After this point the linearity is no longer valid.

$$R = \frac{I_p}{P} \tag{7}$$

The second important parameter is the quantum efficiency which stands for the ratio of the number of produced electrons, N_e, to the number of stricken photons, N_p.

$$\eta = \frac{N_e}{N_p} \tag{8}$$

It is well known that the photocurrent is the number of electrons, N_e, flowing per time, t. It is also known that the light energy is the energy of a photon, E_p, times the number of photons, N_p, over time. If both are combined, it is quite clear that the responsivitiy is proportional with the operating wavelength. This result can be understood more easily by thinking that the light power is inversely proportional with the responsivitiy as shown in Eq. 7-11. More clearly the longer the wavelength, the greater the amount of current produced from the same amount of light power.

$$I_p = \frac{N_e}{t} \tag{9}$$

$$P = \frac{N_p E_p}{t} \tag{10}$$

$$R = \frac{I_p}{P} = \frac{\left(\frac{N_e}{t}\right)}{\left(\frac{N_p E_p}{t}\right)} = \left(\frac{N_e}{N_p}\right)\left(\frac{\lambda}{hc}\right) \tag{11}$$

Another important parameter of a photodiode is the bandwidth. There are two basic procedures that prevent to reach large bandwidths in a photodiode. The first one is the transit time, τ_{TR}, whose reason is the charge carrier's time requirement to produce current. In the Eq. 12, d is the depletion region thickness and the v_{sat}, is the saturation velocity. The second procedure is the depletion capacitance C_d. In the equations listed below; ε is the permittivity of the semiconductor, A is the active area and τ_{RC} is the time constant because of capacitance [15].

$$\tau_{TR} = \frac{d}{v_{sat}} \tag{12}$$

$$C_d = \frac{\varepsilon A}{d} \tag{13}$$

$$\tau_{RC} = R_L Cd \tag{14}$$

If all equations are collected together the bandwidth of the photodiode can be calculated by the Eq. 15 given below.

$$BW_{PD} = \frac{1}{2\pi(\tau_{TR} + \tau_{RC})} \tag{15}$$

There are two types photodiode that are used in modern optical communication systems. First one is the PIN PD and the second one is the APD (Avalanche Photo Diode). APD has excellent linearity over optic power levels ranging from nanowatts to microwatts. More than this values PIN diode provides enough responsivity and SNR for most applications.

2.2.1 PIN Photodiodes

PIN photodiode consist of a thick lightly doped intrinsic or undoped layer sandwiched between thin p and n regions. PIN photodiodes have high quantum efficiency thanks to the large intrinsic layer. So more photons enter this layer and generate more electron-hole pairs than the classic p-n photodiodes. The diffusion current in a PIN PD is very small because the p and n layers are very thin. Because of large intrinsic layer, the reverse voltage can be small. So the result is higher power efficiency. The disadvantage of having such a large intrinsic layer is the bandwidth. According to the Eq. 15, increasing the transit time τ_{TR} has negative effect on PD bandwidth. As we can see on the Fig. 5, PIN PD has extremely large intrinsic layer. The SNR of a PIN PD is given in Eq. 16.

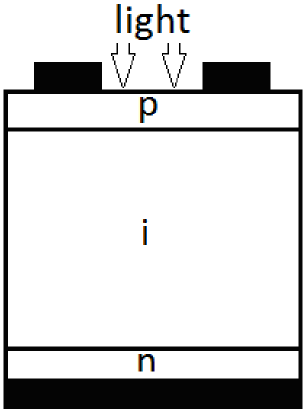

Fig. 5. PIN Photodiode block diagram

$$SNR_{PIN} = \frac{I_p^2}{\sigma^2} = \frac{R^2 P_{in}^2}{(2q)(RP_{in} + I_d)\Delta_f + 4\left(\frac{k_B T}{R_L}\right)F_n \Delta_f} \qquad (16)$$

This type of photodiodes are the most commonly used light detector in fiber optical communication systems because of its easy fabrication, high reliability, low noise, low voltage and relatively high bandwidth [14, 15, 19].

2.2.2 Avalanche Photodiodes

The avalanche photodiode (APD) is a semiconductor junction detector that has internal gain, which increases its responsivity. In this process a photon is absorbed in depletion region to create a free electron-hole pair. Because of the big electrical forces in depletion region, these charges accelerate. Interacting with neutral atoms, charges create additional electron-hole pairs by using a part of their energy to raise electrons across the energy bandgap. One accelerating charge generates several new charges. Secondary charges accelerate and create more and more electron-hole pairs. This is the process of avalanche multiplication. The SNR of APD is given in Eq. 18.

$$R_{APD} = M.R_{PIN} \qquad (17)$$

$$SNR_{APD} = \frac{I_p^{\,2}}{\sigma_S^{\,2} + \sigma_T^{\,2}} = \frac{M^2 R^2 P_{in}^{\,2}}{2qM^2 F_A \left(RP_{in} + I_d \right) \Delta_f + 4\left(\frac{k_B T}{R_L} \right) F_n \Delta_f} \tag{18}$$

If we compare APD and PIN photodiode, the responsivity for an APD is higher than a PIN PD as can be seen in Eq. 17. PIN PD is cheaper, less sensitive to temperature and requires lower reverse bias voltage than the APD. The APD gain is needed when the system is loss limited, as occurs for long-distance links [12, 15, 19].

2.2.3 Noise in Photodiodes

The main sources of noise are dark current noise, shot noise and thermal noise. In an APD, there is one more source of noise due to random nature of avalanche effect. Dark current flows in a circuit when the photodiode is not illuminated. The current amplitude is dependent on the operating temperature, bias voltage and the type of the detector. Shot noise comes from the statistical nature of the generation and collection of photoelectrons when an optical signal comes on photodiode. These statistics are actually modeled by Poisson or Gaussian distribution. Thermal noise is produced in the load resistance. Electrons in a resistor always move because of their thermal energy. This moving is a random process.

2.3 Optical Fibers

The function of an optical communication channel is to transmit the optical signal from transmitter to receiver with minimum distortion.

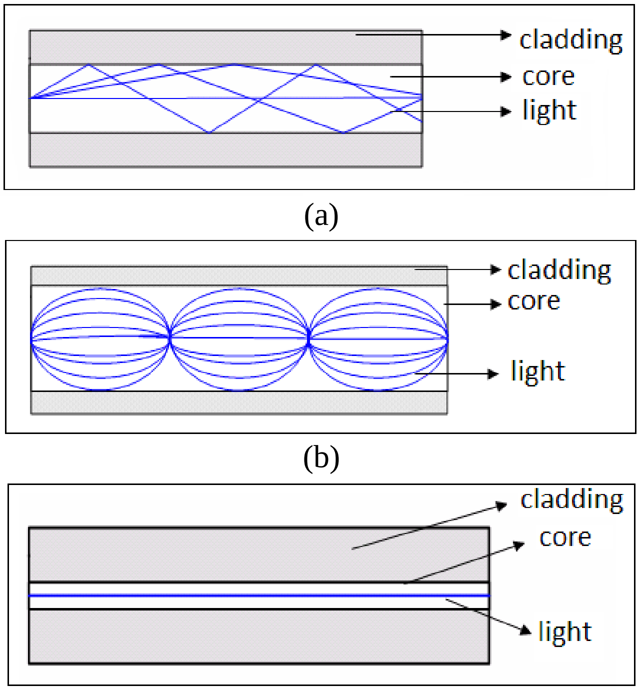

(a)

(b)

(c)

Fig. 6. (a) multimode step index fiber, (b) multimode graded index fiber, (c) single mode fiber

Basically there are three kinds of optical fiber that are being used in fiber optical communication systems showed in Fig. 6. These are step index multimode fiber, graded index multimode fiber and single mode fiber. Step index fiber has only one determined refractive index as single mode fiber but the refractive index of the core in graded index fiber decreases gradually from its center to the cladding to have minimum dispersion effect. In general, the size of a fiber is demonstrated by writing its core diameter and cladding diameter respectively. Single mode fiber has small core in order to have only one mode. This value is about 9 µm. For a step index multimode fiber this value is about 50 µm. Cladding diameter is almost same and around 125 µm for both [15, 19].

2.3.1 Propagation in Optical Fibers

There are basically three theories on the light propagating through a fiber cable. First one is the electromagnetic wave theory. According to the Maxwell equations light can be modeled as an electromagnetic wave and mode is defined as a solution of these equations given Eq. 19-22. Second one is the Quantum theory that describes light as a small energy pack called as photon. The last one is the Ray optics theory which is described by Snell law. All theories are still valid in fiber optical communication systems today.

$$\nabla \mathrm{X} B = \mu_0 J + \mu_0 \varepsilon_0 \frac{\partial E}{\partial t} \tag{19}$$

$$\nabla \mathrm{X} E = -\frac{\partial B}{\partial t} \tag{20}$$

$$\nabla . E = \frac{\rho_v}{\varepsilon_0} \tag{21}$$

$$\nabla . B = 0 \tag{22}$$

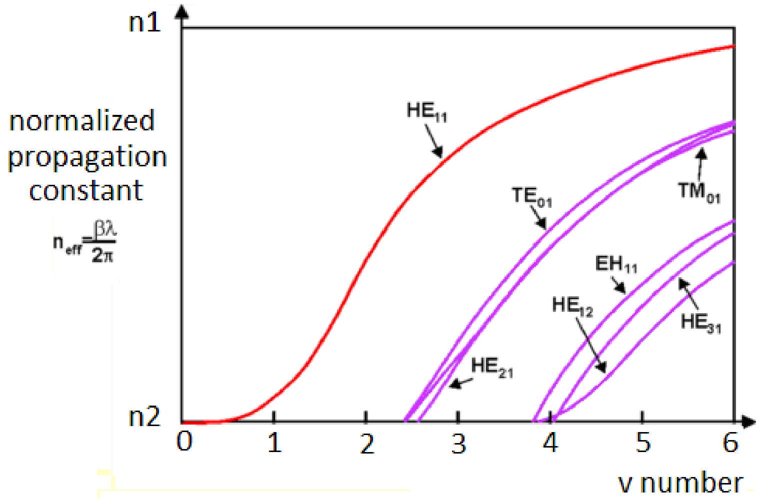

Fig. 7. Normalized propagation constant versus v number

For the electromagnetic wave theory we use mode as an electric field vector rotation. The mode number can be found using the equations given below. Firstly we should find the v number that is shown in Fig. 7. If the v number is smaller than the critical value 2.405 then we can say that we have only one mode propagate through fiber cable. According the Eq. 23 and 24 we can also determine the maximum value of a, to get a single mode along the fiber. Another way to have a single mode along the fiber is to have n_1 and n_2 values very close to each other. Here n_1 and n_2 are the refractive index of the core and cladding respectively.

$$V = \frac{2\pi a}{\lambda}\sqrt{n_1^{\,2} - n_2^{\,2}} \le 2.405 \tag{23}$$

$$a = \frac{2.405.\lambda}{2\pi\sqrt{(n_1^{\,2} - n_2^{\,2})}} \tag{24}$$

For the Ray optics theory light propagate by total internal reflections as denoted in Fig. 8. According to this theory incident rays angle bigger than the α_c can not propagate through the fiber because of the critical incident angle limit [15, 18, 19, 20].

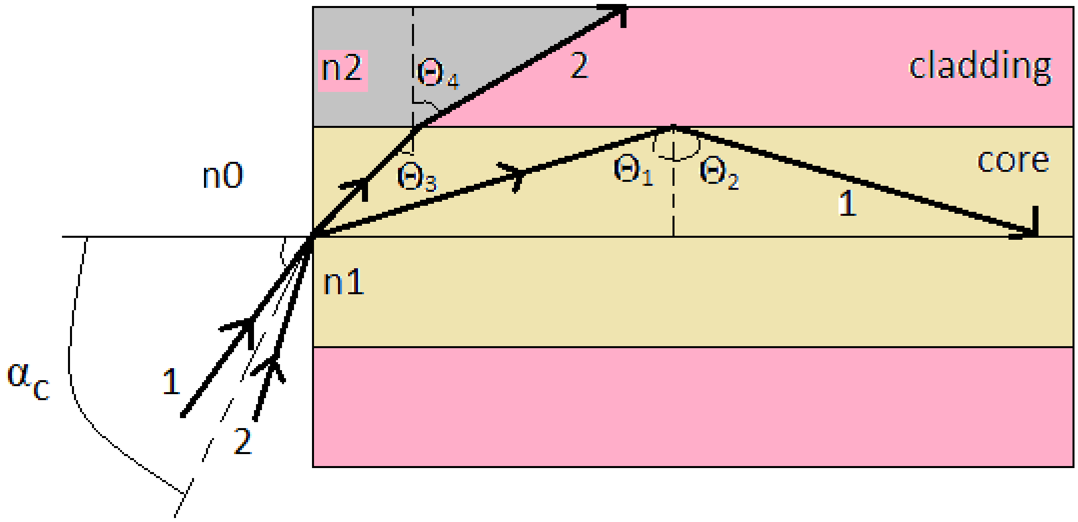

Fig. 8. Ray propagation in a step index fiber

As it can be seen on Fig. 8, ray1 can propagate along the fiber but the ray2 can not. The incident angle where the refraction angle equals to 90 degree is called the critical angle. So the condition incident angle>θ_c must be satisfied to have total internal reflection. Since $\theta_3<\theta_c$, the ray2 can not propagate through the fiber and for ray1 vice versa. The numerical aperture is also related with the acceptance angle α_c can be seen below. Whole procedure can be followed from Eq. 25 to 28.

$$n_1.\sin\theta_3 = n_2.\sin\theta_4 \tag{25}$$

$$\theta_c = \sin^{-1}(n_2 / n_1) \tag{26}$$

$$NA = n_0 . \sin(\alpha_c) = n_1 . \cos(\theta_c) = \sqrt{n_1^{\ 2} - n_2^{\ 2}} \tag{27}$$

$$\alpha_c = \sin^{-1}\left(\frac{\sqrt{n_1^{\ 2} - n_2^{\ 2}}}{n_0} \right) \tag{28}$$

2.3.2 Attenuation in Optical Fibers

Attenuation is the decrease in light power during propagation along a channel. Main attenuation sources are macrobending which is caused by bending the entire optical fiber, microbending which is caused by the imperfection points in fiber optic cable, scattering caused by the same reason with microbending, and absorption due to OH^-. Thanks to Charles K. Kao, most optical communication systems use optical fibers as the communication channel. If the wavelength is suitable, silica fibers can transmit light with losses as small as 0.2 dB/km.

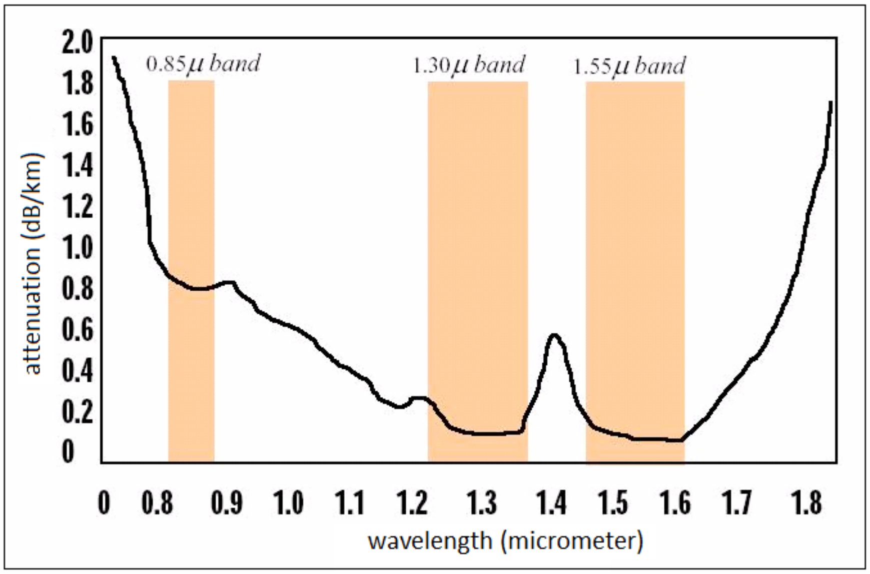

Fig. 9. Attenuation versus wavelength

It can be seen from the Fig. 9 that fiber optical communication can be used three special band denoted above [15, 18, 19, 20, 21].

2.3.3 Dispersion in Multimode Optical Fibers

Multimode fibers carry more than one mode through the fiber cable. Every mode has its own electric field orientation. For that reason every mode has different path along the fiber. The main principle of intermodal dispersion is different rays travel different lengths. As a result these rays disperse in time. The time difference between the first arrived ray and the last arrived ray can be calculated by using Eq. 29. It can be seen on Fig. 10 and Fig. 11 that there are big differences between input signal and output signal due to dispersion and attenuation.

$$\Delta t = \frac{\left(\dfrac{L}{\sin\theta_c} - L \right)}{c/n_1} \tag{29}$$

The dispersion limit comparation for a step index fiber and graded index fiber can be done by focusing on the Eq. 30 and Eq. 31. As it can be seen these equations graded index fibers has bandwidth X length product bigger than step index fibers [19].

$$BL < \frac{n_2}{n_1}\frac{c}{(n_1 - n_2)} \tag{30}$$

$$BL < \frac{8cn_1}{(n_1 - n_2)^2} \tag{31}$$

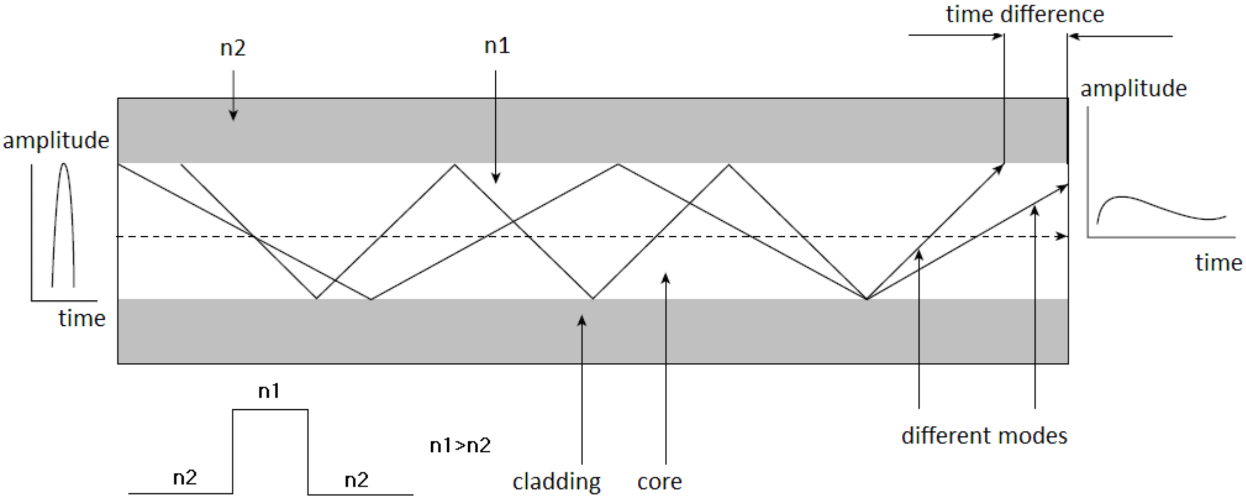

Fig. 10. Multimode dispersion

2.3.4 Dispersion in Single Mode Optical Fibers

Different spectral components of an optical signal travel different speed along the fiber cable. So some parts of the pulse arrive later than the others. This event is known as group velocity dispersion or chromatic dispersion. Two main reasons can be trigger chromatic dispersion. The first one is the material dispersion caused by the wavelength dependent refractive index. The second one is the waveguide dispersion caused by the wavelength dependent mode field distribution. We can not talk about intermodal dispersion in single mode fibers. Because there is only one mode propagate along the single mode fiber cable. Comparing Fig. 10 and Fig. 11, it can be understood easily that single mode fiber is more suitable for long haul fiber optical communication systems than multimode fibers especially for the distance more than 50 km.

$$Vg = \left(\frac{d\beta}{d\omega} \right)^{-1} \tag{32}$$

If we have a pulse with a spectral width is ΔW, the pulse spreading can be calculated using the Eq. 33. Here β_2 is the group velocity dispersion (GVD) parameter. V_g is defined as the group velocity as shown by Eq. 32. If we reorganized these equations using Eq. 34, we can get Eq. 35 and 36 which describe the dispersion parameter presented in the unit of ps/(nm.km) [20].

$$\Delta T = \frac{dT}{d\omega}\Delta\omega = \frac{d}{d\omega}\left(\frac{L}{V_g} \right)\Delta\omega = L\frac{d^2\beta}{d\omega^2}\Delta\omega = L\beta_2\Delta\omega \tag{33}$$

$$\beta_2 = \frac{d^2\beta}{d\omega^2} \tag{34}$$

$$\Delta T = \frac{d}{d\lambda}\left(\frac{L}{V_g} \right)\Delta\lambda = DL\Delta\lambda \tag{35}$$

$$D_t = \frac{d}{d\lambda}\left(\frac{1}{V_g} \right) = -\frac{2\pi c}{\lambda^2}\beta_2 \tag{36}$$

Another dispersion source is the Polarization Mode Dispersion (PMD) which is normally relatively small compared with chromatic dispersion. But if chromatic dispersion is compensated then PMD becomes dominant of the total dispersion. Although single mode fibers carry only one mode, actually there are two modes which are linear-polarized waves that propagate within a fiber in two orthogonal planes. If fiber is not perfect these modes have different velocities. So they can not arrive at the fiber end simultaneously. Finally PMD is occurred. PMD parameter can be calculated using the Eq. 37 in the units of $ps/\sqrt{km}$ [20].

$$\Delta T_{PMD} = D_{PMD}\sqrt{L} \tag{37}$$

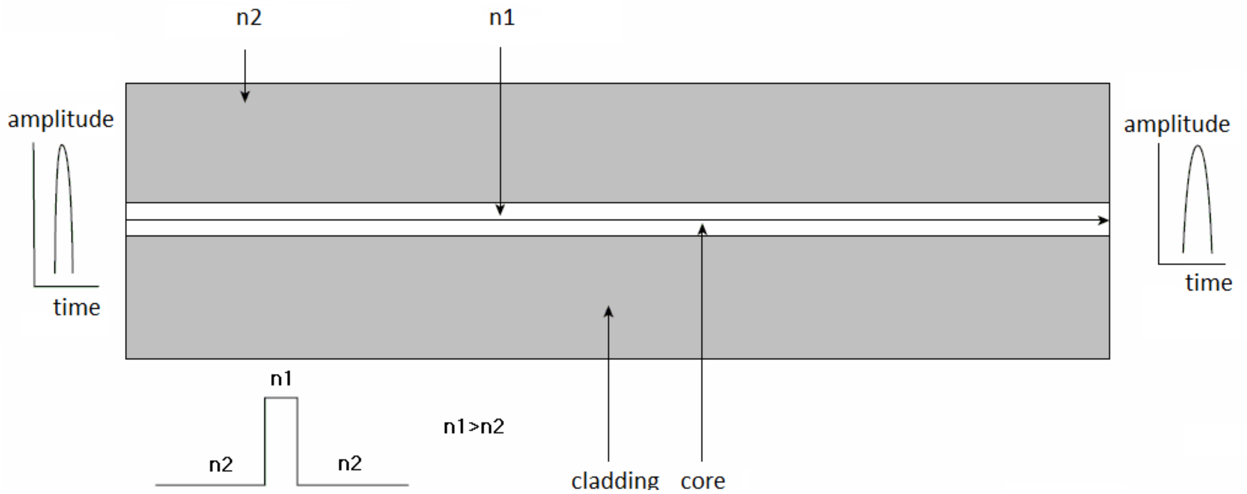

Fig. 11. Multimode dispersion

2.4 Optical Amplifiers

An optical amplifier is a device which amplifies the optical signal directly without changing it to electric signal. The light itself is amplified. There are three types of optical amplifier as shown in the Fig. 12.

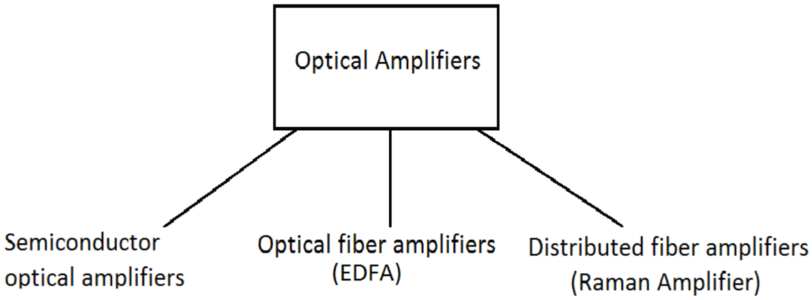

Fig. 12. Types of optical amplifiers

2.4.1 Semiconductor Optical Amplifiers

Semiconductor optical amplifier is an active medium of a semiconductor laser with very low optical feedback. The main problem is that it has been difficult to make SOAs longer than about 450 μm. In this short distance there is not sufficient gain available for one single pass through the device for useful amplification to be obtained. One solution is to retain the reflective facets (mirrors) characteristic of laser operation.

2.4.2 Erbium Doped Fiber Amplifiers (EDFA)

Erbium-Doped Fiber Amplifier (EDFA) is one of the fundamental breakthroughs that allowed long-haul DWDM systems to work more efficiently. At the heart of the EDFA, the fiber is doped with erbium, an earth element that happens to have the appropriate energy levels in its atomic structure for amplifying light at 1550 nm. A 980 nm or 1480 nm pump laser is used to inject energy into the erbium-doped fiber. A significant point is that the erbium gives up its energy in the form of additional photons which are exactly in the same phase and direction as the signal being amplified. There is usually an isolator placed at the output to prevent reflections returning from the attached fiber.

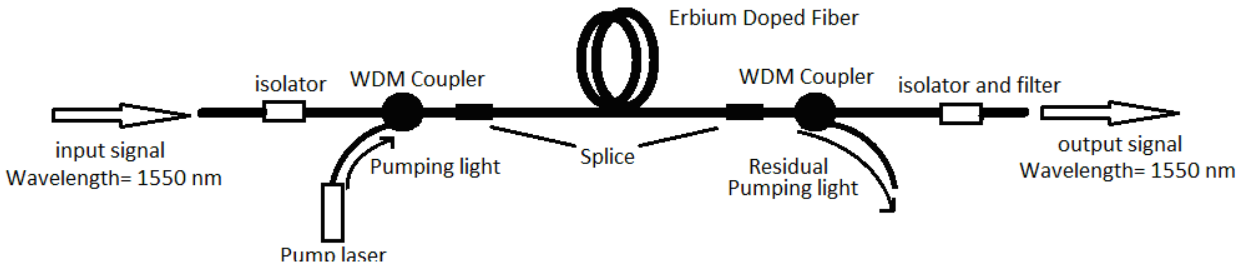

Fig. 13. Erbium Doped Fiber Amplifier

When a signal at 1550 nm enters the fiber, the light stimulates the erbium atoms to release their stored energy as additional 1550 nm light. There are two different wavelengths can be used for pumping. If 980 nm wavelength is used, this is an indirect method. Because, erbium ions move from level 1 to level 3. After nonradiating fast decay as shown on Fig. 14, they come in level 2. After population inversion they fall to level 1 by radiating the expected wavelength (L or C band). If pumping is done directly (1480 nm), only two energy levels are involved. Since lifetime of erbium ions is long enough at level 2, they accumulate here and produce population inversion. This process continues as the signal passes down the fiber, growing stronger and stronger as it goes. The principle involved is the principle of a laser. When an erbium ion is in a high-energy state, a photon of light will stimulate it to give up some of its energy and return to a lower-energy (more stable) state (“stimulated emission”) [15, 18, 19, 20, 21].

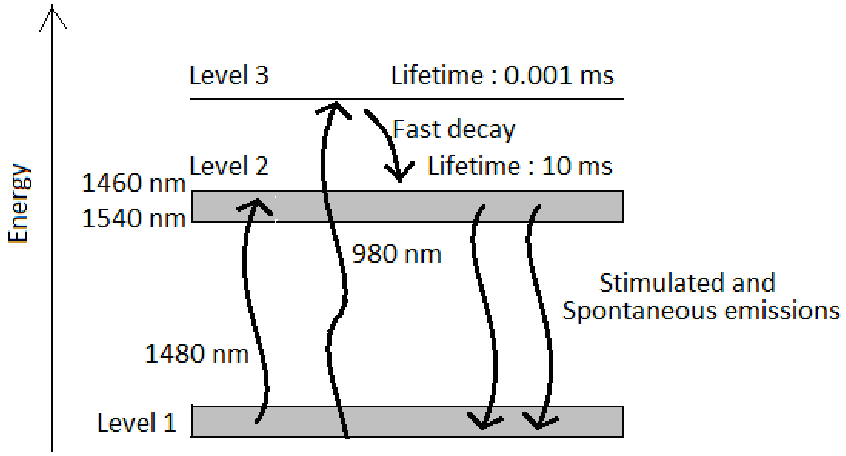

Fig. 14. Energy levels of an Erbium Doped Fiber Amplifier

2.4.3 Raman Amplifiers

Raman amplifiers are used often as preamplifiers to enhance the performance of EDFAs in dense wavelength division multiplexing (DWDM) systems. They are being placed nearly every long-haul fiber-optic transmission systems [22]. Raman gain arises from the transfer of power from one optical beam to another that is downshifted in frequency by the energy of an optical photon. Amplification usually occurs throughout the length of the transmission fiber itself in a process known as distributed amplification, rather than in a discrete amplification, or lumped amplification configuration such as that employed by an erbium-doped fiber amplifier (EDFA). Raman amplification occurs as a high-energy pump wavelength is sent in the reverse direction from the output end of the fiber span, where the incoming signal is weak. The pump wavelength, which generally is in the 1450 nm range (E-Band), interacts with and excites atoms in the crystalline lattice of the fiber core. Atoms absorb the photons, and quickly release photons with energy equal to the original photon, plus or minus atomic vibration. In other words, a frequency/wavelength shift occurs as the pump wavelength propagates along the fiber in the reverse direction. The energy lost in the pump wavelength shifts to longer-wavelength (within about 100 nm) signals, generally in the 1550 nm window (C-Band), in the forward direction, thereby serving to amplify them. Raman amplifiers offer the advantage of amplifying signals in the broad range extending from 1300 nm to 1700 nm. Further, they perform better than EDFAs in terms of signal to-noise ratio (SNR).

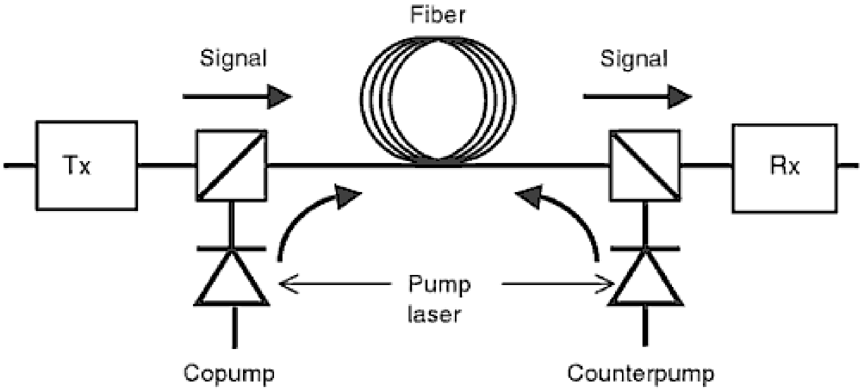

Fig. 15. Schematic of Raman Amplifier

Raman amplifiers have some advantages. First, Raman gain exists in every fiber, which provides a lower cost comparing with the other amplifiers. Second, gain is available almost whole fiber ranging from approximately 0.3 to 2 μm. A third advantage of Raman amplifiers is that the gain spectrum can be changed by arranged the pump wavelengths [22]. Fourth advantage of Raman amplifications is that it is a relatively broad-band amplifier with a bandwidth 5 THz with a flat gain. There are also a number of challenges for Raman amplifiers. Raman amplifiers have poor pumping efficiency at lower signal powers compared to the EDFAs. If one use a Raman amplifier, the fiber length must be longer but this disadvantage can be decreased by using amplification and the dispersion compensation together in a fiber [22].

3 THEORY

3.1. Principle of Orthogonal Frequency Division Multiplexing (OFDM)

OFDM is a special form of multi-carrier modulation. The classical MCM uses non-overlapped band limited signals, and can be implemented with a large number of oscillators and filters for both transmitters and receivers. The main disadvantage of MCM is that it requires a large bandwidth. This is because in order to design the filters and oscillators cost-efficiently, the channel spacing has to be multiple of the symbol rate, greatly reducing the spectral efficiency. A novel approach called orthogonal frequency-division multiplexing (OFDM) is employed to have overlapped orthogonal signal set. This orthogonality comes from the powerful correlation between any two subcarriers.

$$\int_{t=0}^{Ts} f_n(t)\, f_m^{*}(t)dt = \begin{cases} 0, n \neq m \\ 1, n = m \end{cases} = A_n \delta_{nm} \qquad \delta_{nm} = \begin{cases} 0, n \neq m \\ 1, n = m \end{cases} \tag{37}$$

If the following condition is satisfied, then the two subcarriers are orthogonal to each other. This signifies that these orthogonal subcarrier signals, with their frequencies spaced at multiple of inverse of the symbol rate can be recovered without inter-carrier interference (ICI), in spite of strong signal spectral overlapping.

$$\int_{t=0}^{t=T} f_1(t)\, f_2(t) = 0 \tag{38}$$

An OFDM subcarrier can be seen below where C_c is the amplitude of the subcarrier, ϕ_c is the phase of the subcarrier and f_c is the frequency of the subcarrier.

$$S_c(t) = C_c(t).\exp(\, j(2\pi f_c t + \varphi_c(t))) \tag{39}$$

An OFDM symbol is composed of a number of subcarriers as shown following equation where Nsc is the number of subcarriers and $f_n = f_o + n\Delta_f$

$$S_s(t) = \frac{1}{N_{SC}} \sum_{n=0}^{N_{SC}-1} C_n(t).\exp(\, j(2\pi f_n t + \varphi_n(t))) \tag{40}$$

If it is assumed that a subcarrier amplitude and phase doesn’t change during one symbol time and sampling $f_s = 1/T_s$, given by

$$\begin{aligned} C_n(t) &= C_n \\ \varphi_n(t) &= \varphi_n \end{aligned} \tag{41}$$

$$S_s(kT_s) = \frac{1}{N_{SC}} \sum_{n=0}^{N_{SC}-1} C_n \exp(j(2\pi(f_0 + n\Delta f)kT_s + \varphi_n)) \tag{42}$$

Where T_s is the sampling period T_{SYM} is the symbol period shown below.

$$T_{SYM} = N_{SC} T_s \tag{43}$$

Assuming that $f_0=0$ and $\Delta f=1/(N_{SC}.T_s)$, an OFDM symbol can be given by

$$S_s(kT_s) = \frac{1}{N_{SC}} \sum_{n=0}^{N_{SC}-1} C_n.\exp(j2\pi n\frac{k}{N_{SC}}).\exp(j\varphi_n) \tag{44}$$

A fundamental difference of the OFDM is that a large number of subcarriers are needed so that the transmission channel affects each subcarrier as a flat channel. So we need very complex architecture including many oscillators and filters for both transmit and receive end. But, instead of using such a complicated electronic circuit for OFDM modulation/demodulation we can use IFFT and FFT blocks as showed in Fig. 16 [10, 11, 23, 24].

Table 2. IEEE 802.11a basic parameters

Parameter	**Value**
Sampling frequency, f_S	20 *MHz*
Sampling Period, T_S	50 *ns*
Useful symbol duration, T_U	3.2 μs
Cycling prefix duration, T_{CP}	0.8 μs
Symbol duration, $T_{SYM}=T_U+T_{CP}$	4 μs
Data subcarrier number, N_{SD}	48
Pilot subcarrier number, N_{SP}	4
Total subcarrier number, $N_{SC}=N_{SD}+N_{SP}$	52
Subcarrier frequency interval, Δf	0.3125 *MHz*

3.2. Principle of Coherent Optical OFDM (CO-OFDM)

A general diagram of a complete CO-OFDM system can be seen in Fig. 16. The purpose of using the OFDM transmitter is to get the data bits into each OFDM symbol, and generate the time series by the algorithm of inverse fast Fourier transform (IFFT), including insertion of the guard interval, and then up convert to an suitable RF frequency to be fed into an optical link. The function of the MZM is to linearly shift the OFDM spectrum from the RF domain to the optical domain [1-7]. The received optical signal for one OFDM symbol after traversing, can be seen in equation given below.

$$E_s = \exp(j(2\pi(f_{LD1} + f_{LO1})t + \phi_{LD1}))\sum_{n=1}^{Nsc} c_n.\exp(j2\pi.f_n t)exp(j\varphi_D(n)) \tag{45}$$

$$\varphi_D(n) = \frac{1}{2}\beta_2\omega^2 L \tag{46}$$

$$\beta_2 = \frac{\lambda^2}{2\pi c}D_t \tag{47}$$

$$\varphi_D(n) = \frac{v.\pi}{{f_{LD}}^2}D_t {f_n}^2 L \tag{48}$$

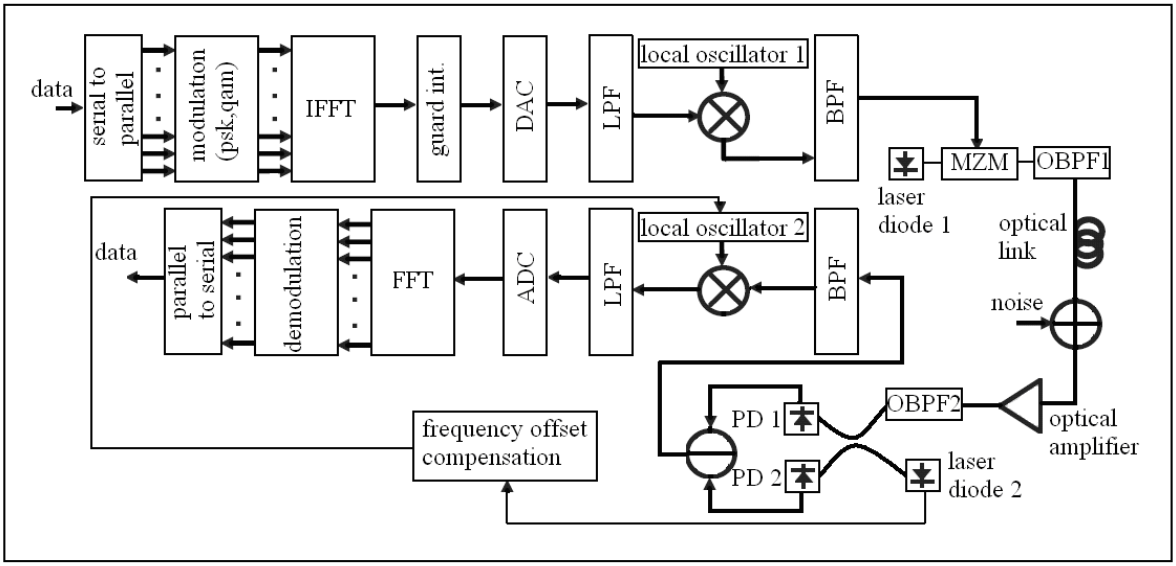

Fig. 16. CO-OFDM block diagram

CO-OFDM system consists of an electrical OFDM transmitter, an OFDM RF to optical up converter, an optical communication link, an OFDM optical to RF down converter and an electrical OFDM receiver as shown in Fig. 16. CO-OFDM has also been shown as the immunity to polarization mode dispersion. Because CO-OFDM utilizes linear RF-to optical up conversion in the transmitter and linear optical-to- RF down conversion in the receiver, we model CO-OFDM transmission as parallel linear channels as shown in Fig. 17. It has been proposed and analyzed that by biasing the Mach- Zehnder modulators (MZMs) at null point, a linear conversion between the RF signal and optical field signal can be achieved [1]. It has also been shown that by using coherent detection, a linear transformation from optical field signal to RF (electrical) signal can be achieved. In order to reach the minimum nonlinearity, as an amplifier, we choose the EDFA assuming with selected properly pump power and suitable excited cable length [25-31].

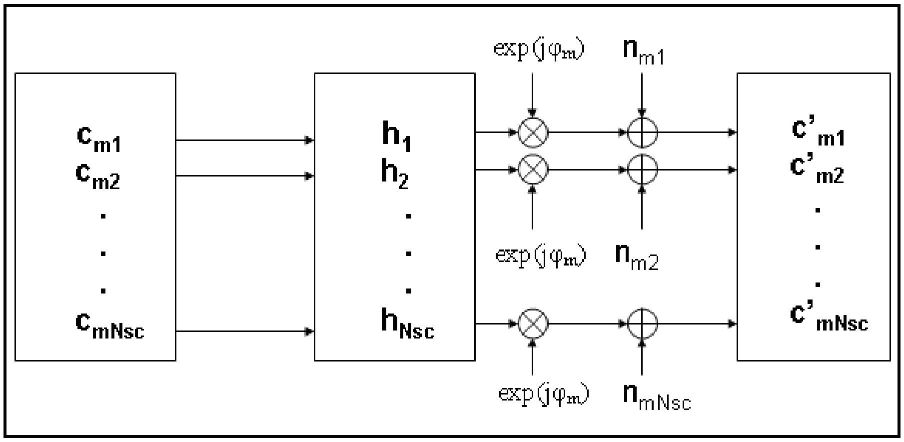

Fig. 17. Optical channel model for single mode optical fiber

$$c'_{mn} = c_{mn}.h_n.\exp(j\varphi_m) + n_{mn} \tag{49}$$

$$h_n = \exp(j(\varphi_0 + 2\Pi\tau_0 f_n + \varphi_D(n))) \tag{50}$$

The group velocity delay consists of a zeroth-order dc term φ_0, a linear term proportional to the time delay of the first subcarrier τ0, and a quadrature term proportional to the fiber chromatic dispersion D_t in the unit of ps/pm for each 1000 km. f_{LD} is the optical carrier frequency and $\varphi_D(n)$ is the phase dispersion of each subcarrier owing to the fiber chromatic dispersion [24-27]. Optical channel model and related equations is given Eq. 49. and Eq. 50 respectively. In these equations; c_{mn} and c'_{mn} are transmitted and received signal respectively, h_n is the transfer function for the nth subcarrier, φ_m is the phase drift of the mth OFDM symbol, and n_{mn} is the white Gaussian noise with zero-mean. The transfer functions of the subcarriers in optical fibers are assumed as static within one OFDM frame. The phase drift within one OFDM symbol can be considered as constant and common to all the subcarriers [28, 29]. We chose 20 kHz linewidth for each laser diode which is close to the value achieved with commercially available. In order to realize a CO-OFDM system, we also have to cope with the phase drift of the carrier. Existence ISI between subcarriers in CO-OFDM system causes disappearing of orthogonality. For that reason a cyclic prefix is added to the OFDM subcarriers. If a cyclic prefix whose extension is long enough from the channel delay spread is added in front of the CO-OFDM symbol, the delay spread that is the effect of chromatic dispersion can not create ISI as given below where v is the light velocity in fiber cable.

$$\frac{v}{{f_{LD}}^2}|D_t|N_{sc}\Delta_f \le \Delta_G \tag{51}$$

Comparing to the direct detection systems, laser phase drift effect is more important issue on CO-OFDM systems. In order to get proper data at receiver side, laser phase drift must be estimated and fixed from the received signal. For that reason pilot carriers added OFDM signal is used as given by,

$$\bar{\varphi}_m = \frac{1}{N_P}\sum_{n=1}^{N_{SP}}[\arg(c'_{mn}) - \arg(c_{mn})] \tag{52}$$

The average of the difference between transmitted and received subcarrier phases will be approximately equal to the average phase shift because of the laser phase drift. After estimating the laser phase drift, phase fixing process is done as given below in Eq. (53-54).

$$\overset{fs}{c}_{mn} = c'_{mn}\exp(-j\bar{\varphi}_m) \tag{53}$$

$$\bar{c}_{mn} = \overset{fs}{c}_{mn}\frac{h_n^{*}}{|h_n|^2} \tag{54}$$

After transmitting 512 symbols the channel profile is estimated over received data or a preamble array. Thanks to the sufficient number of OFDM subcarriers, data rate of each subcarrier is not higher. So, this technique can be used not only for the chromatic compensation, but also for the polarization mode dispersion with higher data rate.

4 RESULTS

In order to get the results of the work, a Monte Carlo computer simulation program was developed [11]. The variables of fiber optical channel were determined based on three parameters. The first one is a phase component whose variation depends on the subcarrier frequency and occurs because of chromatic dispersion, the second one is laser phase noise effect and the last component is the optical noise. Furthermore an attenuation coefficient is about 0.2 dB/km for fiber cable has been taken into consideration. EDFA has been used to eliminate this attenuation factor. Due to its lack of sensitivity of amplitude changing, phase shift keying (PSK) has been chosen for constituting OFDM symbol as a digital modulation technique. Pilots added method has been used for estimating laser phase noise. Optical fiber parameters and basic OFDM parameters are given Table 3 and Table 4 respectively. In order to determine the cable effects, two kinds of dispersion parameters (6 ps/(nm.km) and 17 ps/(nm.km)) are used for the designed Monte Carlo simulation.

In this work, firstly the relation between SNR-BER is obtained for three different data rates showed in Fig. 18. In the second section of the work we get the BER-Distance variations as showed in Fig. 19-20. Finally the constellation diagrams of received data have been obtained. It is well known that BER threshold of 10^{-2} is a sufficient level for advanced Forward Error Correction (FEC) [1, 32].

Table 3. Basic fiber optical parameters

Parameter	Value
Wavelength	1550 nm
Velocity of light in fiber cable	200000 km/s
Fiber optical cable length	100 -1800 km
Chromatic dispersion parameter of fiber (D_t)	6 ps/(nm.km), 17 ps/(nm.km)

Table 4. Basic OFDM parameters for computer simulation (for 16gbps)

Parameter	**Value**
Sampling frequency, f_S	20 GHz
Sampling Period, T_S	50 ps
Useful symbol duration, T_U	25.6 ns
Cycling prefix duration, T_{CP}	3.2ns, 6.4 ns
Symbol duration, $T_{SYM}=T_U+T_{CP}$	28.8 ns, 32ns
Data subcarrier number, N_{SD}	448
Pilot subcarrier number, N_{SP}	64
Total subcarrier number, $N_{SC}=N_{SD}+N_{SP}$	512
Subcarrier frequency interval, Δf	39.0625 MHz

Figures below show that fixing laser phase noise method has at least 3 dB advantage to no fixing method. Fig. 18 demonstrates that if the D_t increases from 6 ps/(nm.km) to 17 ps/(nm.km), SNR decreases 3 dB at 8 Gb/s for the same BER and the same cyclic prefix. Fig. 19 supports the theory that to reach high data rates we need to have higher SNR values. In these figures ideal optical curves mean that the fiber optical channel has no dispersion effect.

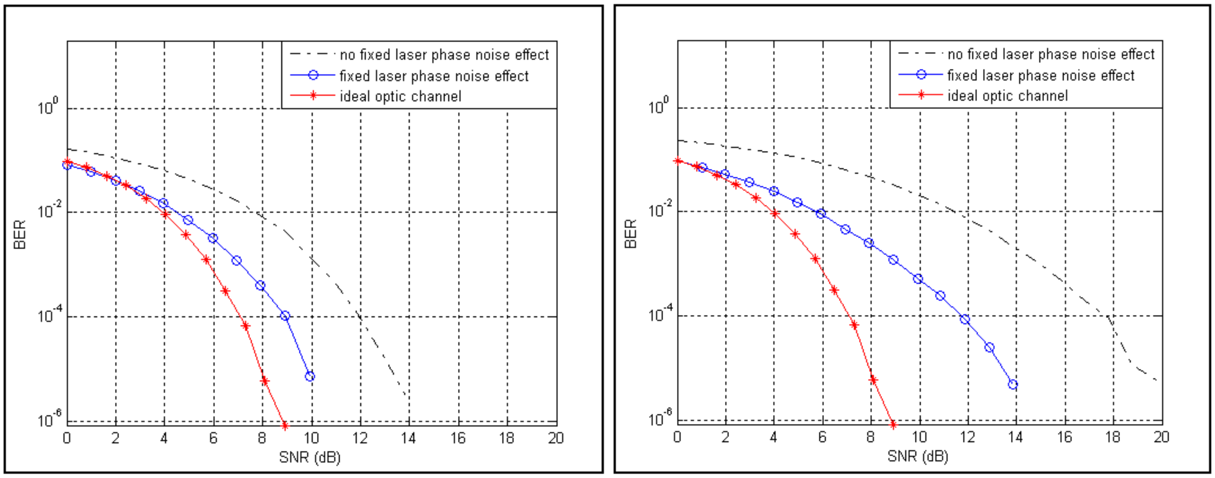

(a) (b)

Fig. 18. SNR-BER performance. (a) 8 Gb/s, D_t: 6 ps/(nm.km), distance: 100 km.(b) 8 Gb/s, D_t: 17 ps/(nm.km), distance: 100 km.

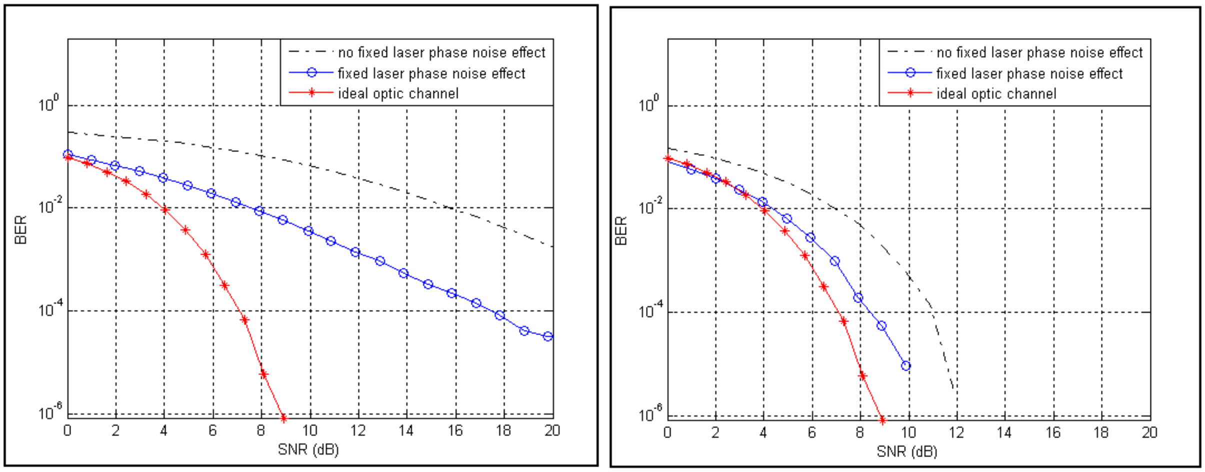

(a) (b)

Fig. 19. SNR-BER performance. (a) 16 Gb/s, D_t: 6 ps/(nm.km), distance: 100km. (b) 5 Gb/s, D_t: 6 ps/(nm.km), distance: 100 km.

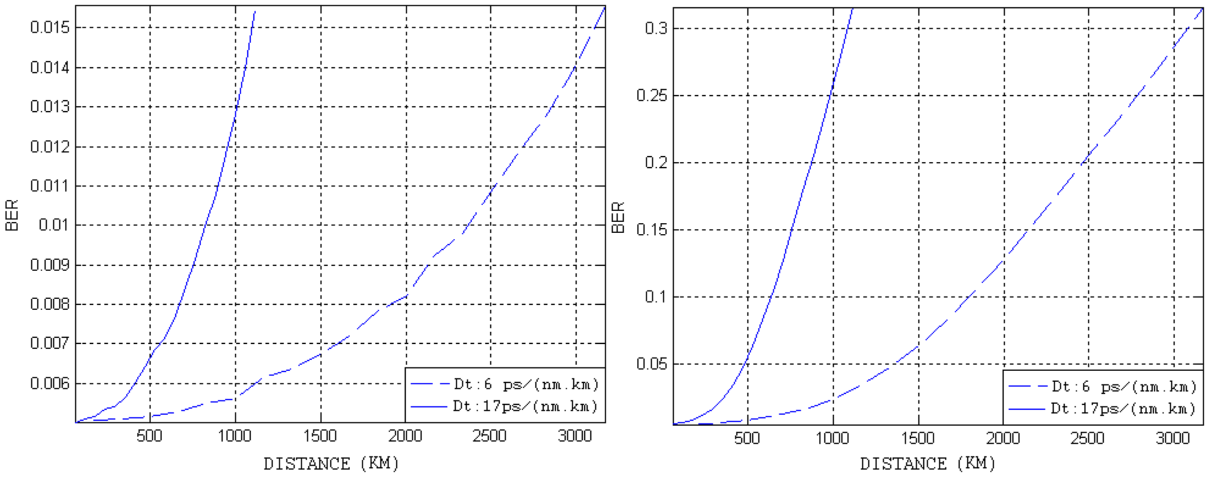

(a) (b)

Fig.20. BER-Distance variation. (a) SNR: 5 dB, Data Rate: 8 Gb/s. (b) SNR: 5 dB, Data Rate: 16 Gb/s

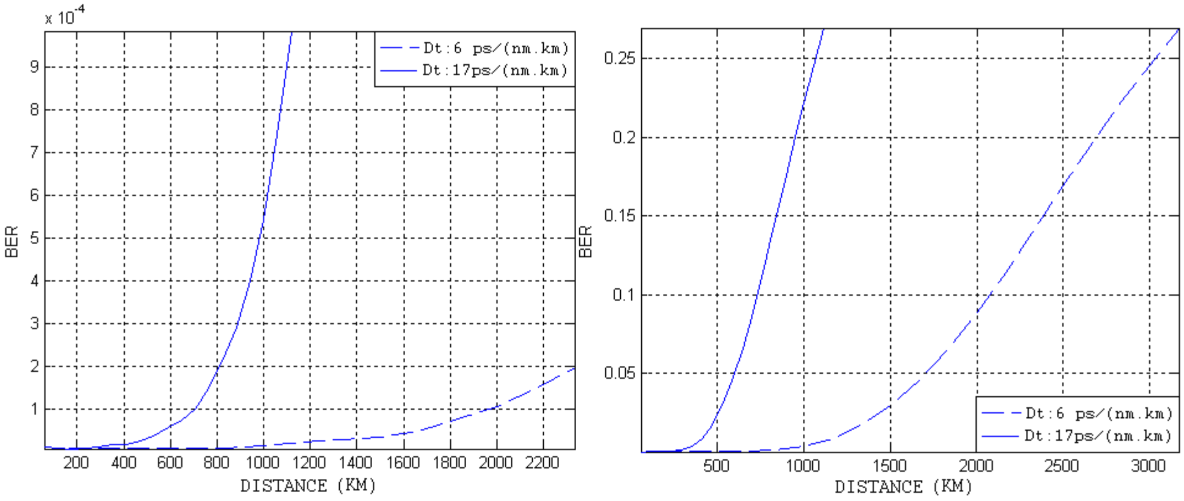

(a) (b)

Fig.21. BER-Distance variation. (a) SNR: 10 dB, Data Rate: 8 Gb/s. (b) SNR: 10 dB, Data Rate: 16 Gb/s.

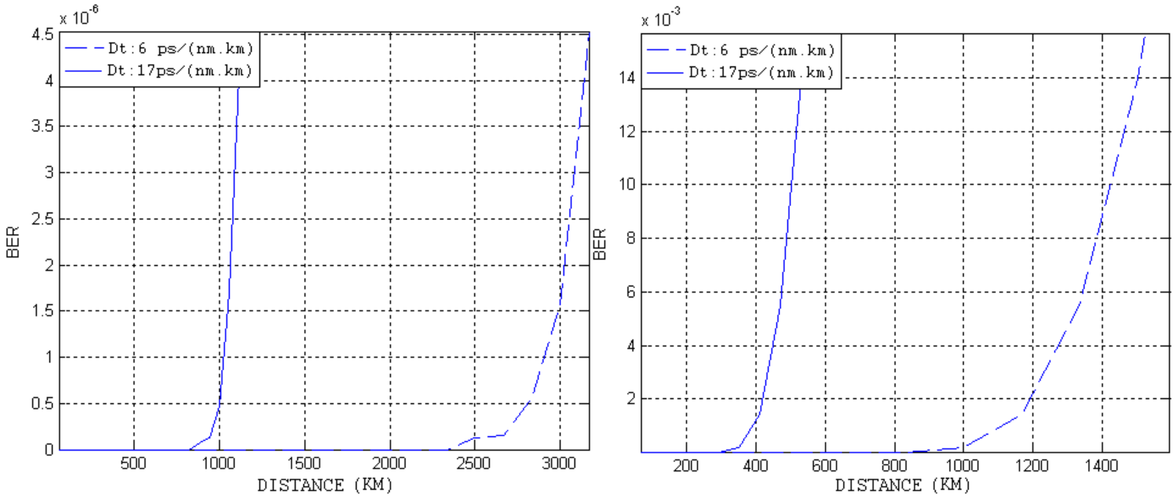

(a) (b)

Fig. 22. BER-Distance variation. (a) SNR: 15 dB, Data Rate: 8 Gb/s. (b) SNR: 15 dB, Data Rate: 16 Gb/s.

According to the graphics obtained, it can be seen in Fig. 20-22, BER values increase exponentially with data rate and link distances. These results support the theory that chromatic dispersion is more effectual in high data rate and long distances. For the fiber optical link design, it is well known that, attenuation is more important in short distance and dispersion is more important in long distance for a fiber optical link. Some values from simulation results selected for designing a sample link may be summarized:

- BER: 10^{-2}, Data Rate: 16 Gb/s, Chromatic Dispersion Parameter: 6 ps/(nm.km); Distances: 600, 1250, 1500 km for SNR: 5, 10, and 15 dB respectively without FEC.

- BER: 10^{-5}, Data Rate: 8 Gb/s, Chromatic Dispersion Parameter: 17 ps/(nm.km); Distances: 295, 1270 km for SNR: 10, 15 dB respectively without FEC.

It is very crucial to know that these results are taken for only one fiber core and one RF carrier. Using WDM and still one RF carrier, system capacity can reach up to 1.7 Tb/s.

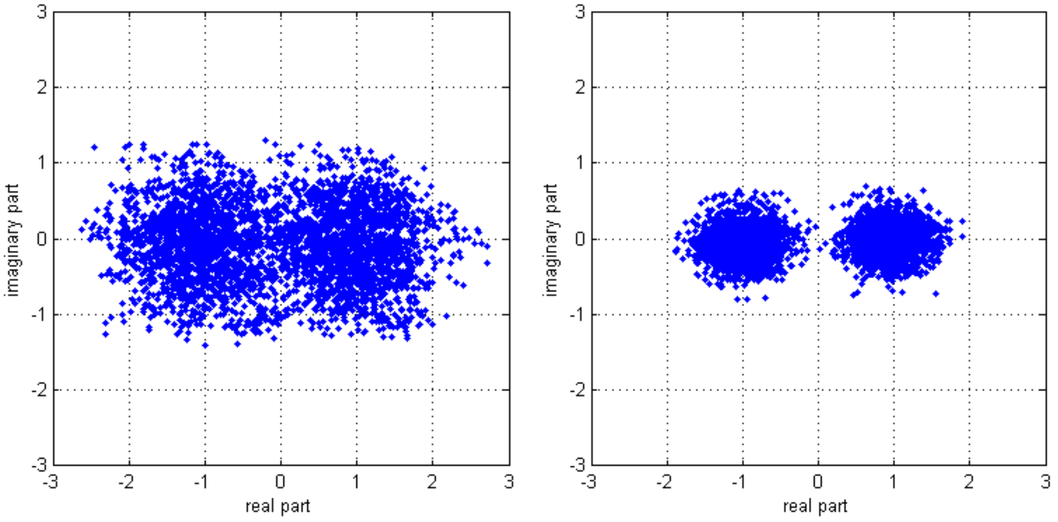

(a) (b)

Fig. 23. Constellation diagrams; 1000 km link distance, 17 ps/(nm.km) dispersion parameter and 8 Gb/s data rate. (a) SNR:3 dB. (b) SNR:10 dB.

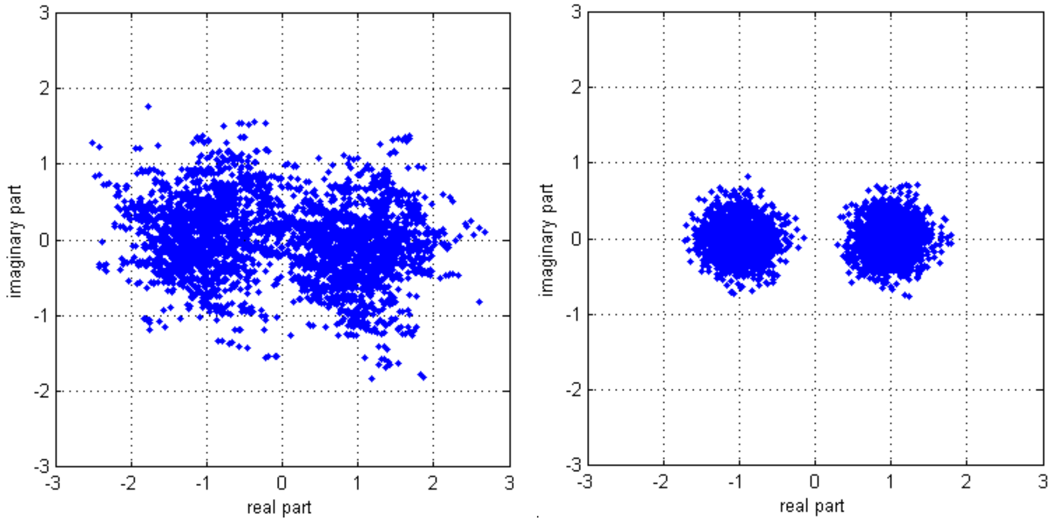

(a) (b)

Fig. 24. Constellation diagrams; 1000 km link distance, 6 ps/(nm.km) dispersion parameter and 8 Gb/s data rate. (a) SNR:3 dB. (b) SNR: 10 dB.

Fig. 23 and Fig. 24 shows constellation diagrams of received BPSK modulated data after removing chromatic dispersion and average phase noise of one OFDM symbol. It can be seen in Fig. 23 and Fig. 24 that switching dispersion parameter from 17 ps/(nm.km) to 6 ps/(nm.km), constellation diagrams show different characteristics. These differences are important points on the BER-SNR performance analysis. We get the similar results if we plot these constellation diagrams for 16 Gb/s and 64Gb/s respectively. The only difference we get is the points are more scattered comparing with 8 Gb/s results.

We also simulated the 20 Gb/s data rate results to show that if we want to have higher data rates, we should upgrade the digital modulation format from BPSK to at least QPSK. Because even we have SNR: 24 dB, the BER can not reach 10^{-2}. This result can be seen in Fig. 25. We also calculated the constellation diagrams for 20 Gbit/s using BPSK digital modulation format. These results are given in Fig. 26. These results also support that increasing SNR, we obtain better BER values.

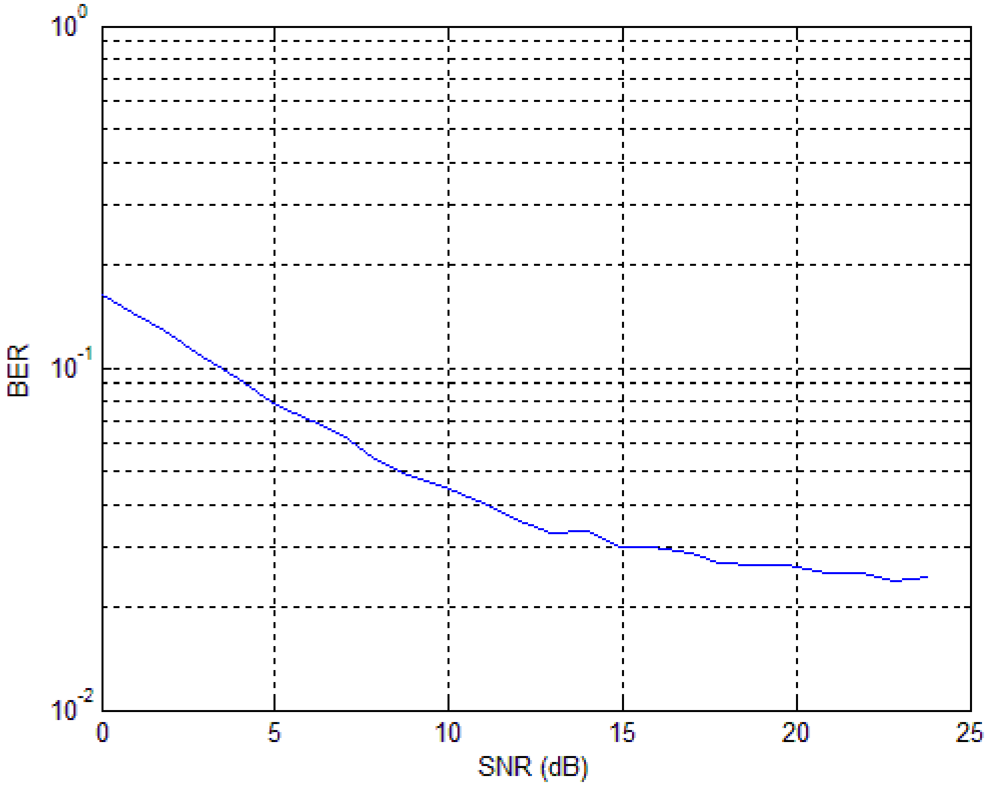

Fig. 25. SNR-BER performance. Data rate: 20 Gb/s, D_t: 6 ps/(nm.km), distance: 1000 km.

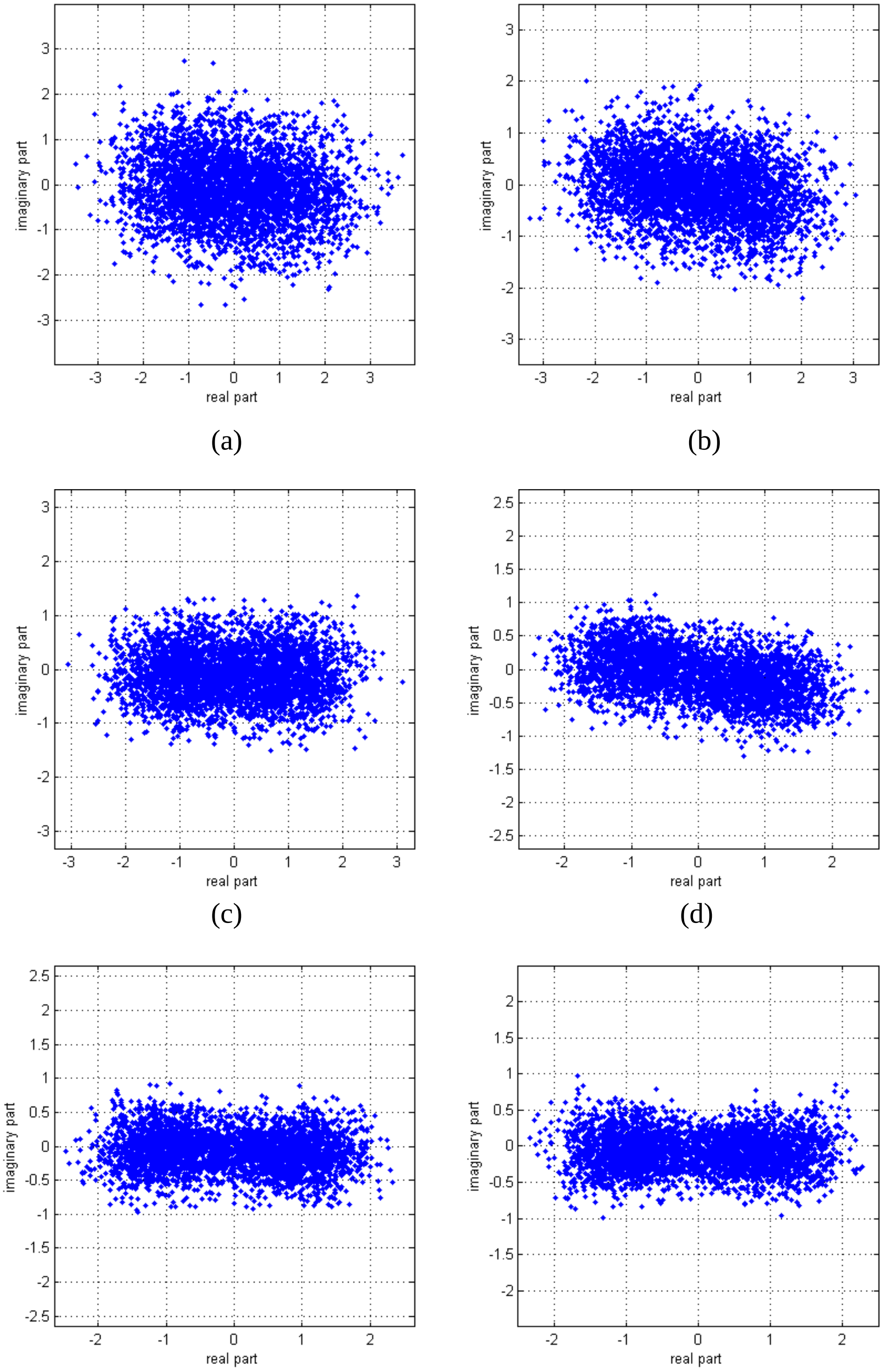

(a) (b) (c) (d) (e) (f)

Fig. 26. Constellation diagrams; 1000 km link distance, D_t: 6 ps/(nm.km) and 20 Gb/s data rate, SNR: a) 0 dB, b) 2 dB, c) 4 dB, d) 6 dB, e) 8 dB and f) 10 dB.

5 CONCLUSIONS

The relation between, data rate, chromatic dispersion, SNR, BER, and link distance are investigated. Simulation results are presented in graphical and also numerical forms. According to the simulation results, some comments and suggestions to design a CO-OFDM link may be given here. For example; If data rate is chosen 8 Gb/s, the link distance can reach up to 700 km for the BER:10^{-4} value (D_t: 17 ps/(nm.km) and SNR: 10 dB). On the other hand if data rate is selected 16 Gb/s, distance can reach up to 400 km with the 10^{-3} BER value (D_t: 17 ps/(nm.km) and SNR: 15 dB). It is very important to know that these values are obtained without using any FEC algorithm. Any solution of these results can be applied for a desired communication link distance as far as minimum nonlinearity conditions satisfied. As we mentioned before, to get high data rates we use two RF carrier instead of one under some limited conditions such as bandwidth of the modulated signal which should not excess the limit of laser bandwidth and the dense spacing limit of the WDM system (if WDM is used). Furthermore we can switch from BPSK to QPSK to get more efficient bits/s/Hz values. In this case we get 64 Gb/s data rate by using same basic structure. This result can increase the data rate up to 6.8 Tb/s (111*64 Gb/s) using only one optical cable and utilizing C and L bands with a good system design. As we mentioned before, it can be seen in Fig. 20-22, BER values increase exponentially with data rate and link distances. These results support the theory that chromatic dispersion is more effectual in high data rate and long distances. For the fiber optical link design, it is well known that, attenuation is more important in short distance and dispersion is more important in long distance for a fiber optical link.

In this work, transmission performance of CO-OFDM is examined and simulated especially at long distances and high data rates. Important parameters such as BER, SNR, distance and bit rate, are examined. Since the chromatic dispersion is an important issue for long haul fiber optical communication systems, its effect is previously observed. The simulation code is renovated under the condition of 15 dB constant SNR to get the tradeoff between BER and link distance which is also a key issue to design optical links with different lengths. We also investigated how the EDFA effect the simulation performance to get a real optical communication simulation. Because of the limited range of the Return Zero (RZ) or On Off Keying (OOK), COOFDM can be used as an alternative solution to increase the link distance between repeaters at high data rates. Simulation based investigations show that CO-OFDM is able to efficiently eliminate the chromatic dispersion in electrical domain if the laser phase noise is properly compensated.

REFERENCES

[1] Djordjevic, I. B. and Vasic, B., Orthogonal Frequency Division Multiplexing for High-speed Optical Transmission, Optical Society of America, Optics Express, 14, 9 2006, 3767.

[2] Shieh, W. and Athaudage, C., Coherent Optical Orthogonal Frequency Division Multiplexing, IEE Electronic Letters, 42, 10 2006.

[3] Bao, H. and Shieh, W., Transmission Simulation of Coherent Optical OFDM Signals in WDM Systems, Optical Society of America, Optics Express, 15, 8 2007, 4410.

[4] Yi, X., Shieh, W. and Tang Y., Phase Estimation for Coherent Optical OFDM, IEEE Photonics Technology Letters, 19, 12 2007.

[5] Jansen, S. L., Morita, I., Takeda N. and Tanaka, H., 20-Gbps OFDM Transmission over 4,160-km SSMF Enabled by RF-Pilot Tone Phase Noise Compensation, Optical Society of America, 2007.

[6] Lowery, A. J., Du L. and Armstrong, J., Orthogonal Frequency Division Multiplexing for Adaptive Dispersion Compensation in long Haul WDM Systems Optical Society of America, 2006.

[7] Tang, J. M. and Shore K. A., 30 Gbps Signal Transmission Over 40 km Directly Modulated DFB Laser Based Single Mode Fiber links Without Optical Amplification and Dispersion Compensation, IEEE Journal of Lightwave Technology, 24, 6 2006.

[8] Chris R. S. Fludger, Thomas Duthel, Dirk van den Borne, Christoph Schulien, Ernst-Dieter Schmidt, Torsten Wuth, Jonas Geyer, Erik De Man, Giok-Djan Khoe, Huug de Waardt, Coherent Equalization and POLMUX-RZ-DQPSK for Robust 100-GE Transmission, Journal of Lightwave Lechnology, 26,1, 2008.

[9] Laude, J. P., DWDM Fundamentals, Components and Applications (Artech house, London 2002.

[10] Microsoft Visual Studio Programming tool.

[11] Yazgan A., Tugcu E., Aydemir Ö. Simsek C., Performance analysis of OFDM systems on AWGN channels, Akademik Bilişim 2009, Turkey.

[12] Tang Y., Shieh W., Yi X. and Evans R., "Optimam Design for RF-to Optical Up-Converter in Coherent Optical OFDM Systems", IEEE Photonic Technology Letters, Vol.19, No.7, April 1, 2007.

[13] Tang Y., Shieh W., and Krongold B. S. "Fiber Nonlinearity Mitigation in 428-Gb/s Multiband Coherent Optical OFDM Systems" Optical Society of America, 2010.

[14] S.M.Sze and Kwok K. Ng. "Physics of Semiconductor Devices Third Edition", John Wiley Sons inc., 2006.

[15] Djafar K. Mynbaev and Lowell L. Scheiner, "Fiber-Optic Communications Technology", Prentice Hall, 2001.

[16] Schubert E. F. "Light-Emitting Diodes Second Edition" Cambridge University Press, New York, 2006.

[17] Benlachtar Y., Watts P. M., Bouziane R., Milder P. A., Rangaraj D., Cartolano A., Koutsoyannis, R., Hoe J. C., Püschel M., Glick M., and Killey R.I. "Generation of optical OFDM signals using 21.4 GS/s real time digital signal processing" Optics Express, Vol. 17, No. 20 Sep 2009.

[18] Franz, J. H. and Jain, V. K., Optical Communications Components and Systems, Alpha Science International Ltd, 2000.

[19] Halmstad University Computer science and Engineering and Electrical Engineering Department, Optical Communications and Solid State Electronics course notes 2010.

[20] Govind P. Agrawal, “Fiber-Optic Communication Systems Third Edition”, John Wiley Sons inc., 2002.

[21] Rajiv, R. and Kumar N. S., Optical Networks a practical perspective Second Edition Morgan Kaufmann Publishers, 2002.

[22] Mohammed N. Islam, “Raman Amplifiers for Telecommunications”, IEEE Journal Of Selected Topics In Quantum Electronics, Vol. 8, No. 3, May/June 2002.

[23] McClellan, J.H., Schafer, R.W. and Yoder, M.A., Signal Processing First, Pearson Prentice Hall, 2003.

[24] Soysal B., High performance receiver design for OFDM based wireless communication systems, PhD Thesis, Karadeniz Technical University Department of Electrical-Electronics Engineering, Trabzon, 2004.

[25] Shieh, W., Bao H. and Tang, Y., Coherent Optical OFDM theory and design, Optical Society of America , Optics Express, 16, 2 2008, 841.

[26] Lowery, A. J. Fiber nonlinearity pre and post compensation for Long optical links using OFDM, Optical Society of America, Optics Express, 15, 20 2007, 12965.

[27] Shieh, W. PMD Supported Coherent optical OFDM Systems, IEEE Photonics Technology Letters, 19, 3 2007.

[28] Bülow, H., Buchali, F. and Klekamp, A., Electronic Dispersion Compensation, Journal of Lightwave Technology, 26, 1 2008.

[29] Tang, J. M., Lane P. M. and Shore K. A., “Transmission Performance of Adaptively Modulated Optical OFDM Signals in Multimode Fiber Links”,IEEE Photonic Technology letters, 18, 1 2006.

[30] Lowery, A. J. and Armstrong, J., Orthogonal Frequency Division Multiplexing for Dispersion Compensation of long Haul Optical Systems, Optical Society of America, Optics Express, 14, 6 2006, 2079.

[31] Shieh, W., Tucker, R. S., Chen, W., Yi, X., and Pendock, G., Optical performance monitoring in coherent optical OFDM systems, Optical Society of America, Optics Express, 16, 2 2007, 350.

[32] Mizuochi T., Miyata Y., Kobayashi T., Ouchi K., Kuno K., Kubo K., Shimizu K., Tagami H., Yoshida H., Fujita H., Akita M. and Motoshima K., “Forward Error Correction based on block Turbo Code with 3-bit soft decision for 10 Gb/s optical Communication systems”, IEEE Journal of Selected Topics in Quantum Electronics, Vol.10, No.2, March 2004.